Published in final edited form as:
Cell Metab. 2008 October ; 8(4): 301–309. doi:10.1016/j.cmet.2008.08.015.

Ablation of CD11c-positive cells normalizes insulin sensitivity in obese insulin resistant animals

David Patsouris[1,4], **Ping-Ping Li**[1,4], **Divya Thapar**[1], **Justin Chapman**[2], **Jerrold M. Olefsky**[1], and **Jaap G. Neels**[1,3,*]

1*Division of Endocrinology & Metabolism, Department of Medicine, University of California, San Diego, La Jolla, California, USA*

2*Pfizer Inc., San Diego, California, USA*

SUMMARY

Obese adipose tissue is characterized by infiltration of macrophages. We and others recently showed that a specific subset of macrophages is recruited to obese adipose and muscle tissue. This subset expresses CD11c and produces high levels of pro-inflammatory cytokines that are linked to the development of obesity-associated insulin resistance. We used a conditional cell ablation system, based on transgenic expression of the diphtheria toxin receptor under the control of the CD11c promoter, to study the effects of depletion of $CD11c^+$ cells in obese mouse models. Our results show that $CD11c^+$ cell depletion results in rapid normalization of insulin sensitivity. Furthermore, $CD11c^+$ cell ablation leads to a marked decrease in inflammatory markers, both locally and systemically, at the level of gene expression and protein levels. Together, these results indicate that these $CD11c^+$ cells are a potential therapeutic target for treatment of obesity-related insulin resistance and type II diabetes.

INTRODUCTION

Over the past decade, it has become quite clear that obesity gives rise to a state of chronic, low-grade inflammation that contributes to insulin resistance (IR) and type-2 diabetes (reviewed in (Shoelson et al., 2007)). In both humans and rodents, adipose tissue macrophages (ATMs) accumulate in adipose tissue (AT) with increasing body weight, and evidence is mounting that implicates ATMs as a significant contributor to inflammation in obesity and a mediator of IR (Shoelson et al., 2007). Several recent studies showed that a decrease in ATMs is associated with a decrease in adipose tissue inflammation and a reduction in obesity-induced insulin resistance (Ellacott et al., 2007; Kanda et al., 2006; Lesniewski et al., 2007; Nara et al., 2007; Neels and Olefsky, 2006; Nomiyama et al., 2007; Weisberg et al., 2006), while an increase in ATMs is associated with a further deterioration of insulin sensitivity (Hirasaka et al., 2007; Kamei et al., 2006; Kanda et al., 2006). Moreover, we showed that disabling the inflammatory pathway within macrophages by creating a myeloid cell-specific knockout of IκB kinase β (IKK-β) or JNK1 protected mice from diet-induced insulin resistance (Arkan et

*__Corresponding author:__ Jaap G. Neels, Inserm U907, Faculté de Médecine, Université de Nice-Sophia Antipolis, 28 Avenue de Valombrose (7ème étage), 06107 Nice, France. Phone: ++ 33 (0) 4 93 37 77 96; Fax: ++ 33 (0) 4 93 81 54 32; E-mail: Jaap.Neels@unice.fr.
[3]Present address: INSERM U907, Faculté de Médecine, Université de Nice-Sophia Antipolis, Nice, France.
[4]These authors contributed equally to this work.

al., 2005; Solinas et al., 2007). Resident tissue macrophages display tremendous heterogeneity in their activities and functions, primarily reflecting the local metabolic and immune microenvironment (Gordon and Taylor, 2005; Mantovani et al., 2004). Recent studies show that there is heterogeneity in ATMs, depending on the lean or obese state (Brake et al., 2006; Lumeng et al., 2007; Nguyen et al., 2007). We and others found two populations of $F4/80^+CD11b^+$ macrophages in AT, one of which also expressed CD11c and accounted for the majority of the increased ATMs on HFD. These studies suggest that $F4/80^+CD11b^+CD11c^+$ cells are a specific population of ATMs recruited to AT upon HFD exposure.

$CD11c^+$ ATMs overexpressed pro-inflammatory cytokines compared with $CD11c^-$ ATMs (Lumeng et al., 2007; Nguyen et al., 2007). In contrast, $CD11c^-$ ATMs expressed high levels of the anti-inflammatory cytokine IL-10, while $CD11c^+$ ATMs exhibited no detectable levels of IL-10 (Nguyen et al., 2007). In addition, we demonstrated that $CD11c^+$, and not $CD11c^-$ cells, are targets for free fatty acid (FFA)-mediated increases in inflammatory responses (Nguyen et al., 2007). Together, these findings suggest that the $CD11c^+$ subset of ATMs plays a major role in the increased expression of pro-inflammatory cytokines in obese AT that can inhibit insulin action, providing a link between inflammation and IR (Shoelson et al., 2007). We therefore hypothesized that specific ablation of $CD11c^+$ immune cells in obese mice would result in a reduction of pro-inflammatory macrophages in obese AT, which could potentially alleviate the IR observed in obesity.

To achieve this, we took advantage of a conditional ablation system mediated by diphtheria toxin (DT) receptor (illustrated in Supplementary Fig. 1; (Jung et al., 2002)). This system relies on the fact that the mouse DT receptor binds DT poorly compared with the simian molecules. Thus, transgenic expression of the simian DT receptor (DTR) confers sensitivity to DT and permits ablation *in vivo* when DT is injected. Transgenic mice that express the simian DTR under the control of the CD11c promoter were previously described (Jung et al., 2002). Immunohistochemical and flow cytometric analysis of these mice revealed DT-inducible depletion of $CD11c^+$ cells in spleen, lymph node, lung, liver and lamina propria tissues, within 18 hours after DT administration (Probst et al., 2005). While transient DC depletion was not associated with signs of illness or long-term defects, repeated DT induction is lethal to the mouse (Jung et al., 2002). However, when wild-type C57BL/6 mice were reconstituted with bone marrow from CD11c-DTR mice and were treated with the same dose of DT, no deleterious effects were observed in these chimeric animals, even with prolonged DT treatment (Zammit et al., 2005). This result suggested that in the CD11c-DTR transgenic mice (Probst et al., 2005) essential nonhematopoietic cells expressed the transgene and were affected by DT treatment. Therefore, we generated chimeric mice, reconstituted with either CD11c-DTR or wild-type (control) bone marrow, and used these for all of our studies (illustrated in Supplementary Fig. 1b).

Using this system, we demonstrate that depletion of CD11c-positive cells results in a marked reduction in macrophages in obese AT and muscle. As expected, this reduction in tissue macrophages is accompanied by both a local and systemic decrease in pro-inflammatory cytokine levels. Furthermore, ablation of $CD11c^+$ cells in obese insulin resistant mice leads to a rapid normalization of insulin sensitivity, in AT, but also in muscle and liver.

RESULTS AND DISCUSSION

Ablation of $CD11c^+$ cells leads to a reduction of crown-like structures in epiWAT

To study the effects of depletion of $CD11c^+$ cells on adipose tissue inflammation and glucose homeostasis in lean and HFD-induced obese mice, we generated chimeric CD11c-DTR mice by transplanting bone marrow from CD11c-DTR transgenic donor mice into lethally irradiated

wild-type (WT) C57BL/6J recipient mice (illustrated in Supplementary Fig. 1). We also transplanted the bone marrow from WT C57BL/6J donor mice back into irradiated WT C57BL/6J recipient mice to control for potential effects of irradiation and non-specific effects of DT treatment. After 6 weeks recovery and reconstitution of the bone marrow, the mice were either fed normal chow (NC; 12% fat) or HFD (60 % fat). After 16 weeks of diet, both the WT and CD11c-DTR bone marrow transplant (BMT) mice were injected i.p. with 10 ng/g bodyweight of DT every other day for different periods of time depending on the experiment (illustrated in Supplementary Fig. 1). Fig. 1a shows that HFD-fed BMT mice gained about 10 grams more weight than NC-fed mice and there were no differences in weight gain between WT and CD11c-DTR BMT mice before the start of DT treatment.

During DT treatment the HFD-fed mice experienced a small degree of weight loss (Supplementary Fig. 2). This was most likely due to the stress induced by the procedures that these animals underwent (e.g. DT injections every other day, clamp surgeries and clamps (see below)), and was not different from weight loss we observed using similar procedures in other unrelated DIO mouse models (data not shown). Furthermore, this minor weight loss was the same regardless of BM genotype and, therefore, is unlikely to contribute to the differential phenotypes attributed to $CD11c^+$ cell depletion.

The increase in whole-body weight on HFD was due to an increase in body fat since both subcutaneous white adipose tissue (SQ-WAT) and epididymal WAT (epi-WAT) depots were increased by 6- and 7-fold, respectively, in DT treated HFD- compared to NC-fed mice. Overall, there were no differences in tissue weights between the two BM genotypes after DT treatment. To determine the effectiveness of DT treatment in depleting $CD11c^+$ ATMs, we isolated the stromal vascular fraction (SVF) of epi-WAT depots from the mice after 3, 5, 9 or 17 days DT treatment, and quantified the proportions of $CD11c^+$ and $F4/80^+CD11b^+CD11c^+$ stromal vascular cells (SVCs) by FACS analyses. Since we observed similar differences in cell proportions regardless of the number of days of DT treatment, we show the combined data of the different treatment groups.

As shown in Fig. 1b, in DT-treated WT BMT mice HFD led to a 2- to 3-fold increase in the percentage of $CD11c^+$ SVCs compared to NC-fed mice. This is in agreement with previous reports (Lumeng et al., 2007;Nguyen et al., 2007). However, in DT-treated CD11c-DTR BMT mice we could only detect background levels ($< 3\%$) of $CD11c^+$ SVCs, regardless of diet. Thus, DT treatment was effective in depleting the epi-WAT of $CD11c^+$ cells.

Previously, ATMs were shown to cluster around dead adipocytes in so-called crown-like structures (CLS; (Cinti et al., 2005; Strissel et al., 2007), and $CD11c^+$ cells are localized to these ATM clusters (Lumeng et al., 2007). Therefore, we performed MAC-2 immunohistochemistry on paraffin sections of epi-WAT to stain ATMs and quantify the number of CLS. Again, we obtained similar results regardless of the number of days of DT treatment and, therefore, show the combined data for all treatment groups. As shown in Fig. 1c, there was a 16-fold increase in the number of CLS in HFD- compared to NC-fed, DT-treated, WT BMT mice, and this increase was markedly (70%) attenuated in the CD11c-DTR BMT mice. Figure 1d shows examples of MAC2 staining, illustrating the quantitative data shown in Fig. 1c.

Ablation of CD11c-positive cells normalizes insulin sensitivity in obese insulin resistant mice

Next, we investigated the effect of $CD11c^+$ cell depletion on glucose homeostasis and insulin sensitivity. Insulin tolerance tests before DT treatment show that HFD-induced obesity resulted in insulin resistance (decreased glucose lowering effect of insulin) in both WT and CD11c-DTR BMT mice, and this effect was greatly attenuated in CD11c-DTR BMT mice 24 hours

after DT treatment (Fig. 2a). Thus, after DT treatment the HFD-fed CD11c-DTR BMT mice were equally insulin sensitive as the chow fed controls.

We also performed glucose tolerance tests (GTTs) and made similar observations (Fig. 2b). HFD induced obesity led to glucose intolerance to the same extent in both WT BMT and CD11c-DTR BMT mice, and DT treatment normalized glucose intolerance in the HFD-fed CD11c-DTR BMT mice within 24 hours.

To investigate whether the effects of $CD11c^+$ cell depletion are specific to HFD-induced obesity, we performed similar experiments in NC-fed leptin-deficient Ob/Ob mice. The Ob/Ob mice were transplanted with WT or CD11c-DTR transgenic bone marrow and underwent DT treatment. ITT and GTT studies demonstrate that $CD11c^+$ cell depletion leads to improved insulin sensitivity in this genetic mouse model of obesity (Supplementary Fig. 3a and b). Furthermore, qPCR analysis of adipose tissue mRNA shows a significant decrease in the expression of the macrophage markers F4/80, CD11b, CD11c and the MCP-1 receptor CCR2 in the WAT of Ob/Ob CD11c-DTR BMT mice compared to their WT counterparts, illustrating a significant reduction of ATMs after DT treatment (Supplementary Fig. 3c–f). Taken together, these results indicate that $CD11c^+$ cell ablation markedly normalizes glucose and insulin tolerance in both HFD-fed and genetically obese mice.

We performed euglycemic clamp studies, to extend the observations made in DT-treated mice and to quantify the insulin sensitivity of muscle (i.e. insulin-stimulated glucose disposal rate), liver (i.e. insulin-mediated suppression of hepatic glucose output) and adipose tissue (i.e. insulin-induced suppression of plasma FFAs). Since we did not observe any differences between BM genotypes before DT treatment in both ITTs and GTTs, we focused our clamp studies on DT-treated mice. WT BMT and CD11c-DTR BMT mice fed normal chow and treated with DT for 14 days did not display any differences in muscle, liver, or adipose tissue insulin sensitivity, confirming our GTT/ITT data showing that $CD11c^+$ cell ablation does not affect insulin sensitivity in NC-fed non-obese mice (Fig. 2c). However, in HFD-fed CD11c-DTR BMT mice treated with DT for 1, 3, or 7 days, we observed normalization of muscle, liver, and adipose tissue insulin sensitivity when compared to their HFD-fed WT counterparts, indicating that $CD11c^+$ cell depletion protects from HFD-induced insulin resistance. Since, the data for the three different durations of DT treatment were comparable, we show the pooled data in Fig. 2c. More specifically, HFD-fed DT treated CD11c-DTR BMT mice have a ~3-fold higher insulin-stimulated glucose disposal rate (IS-GDR) (24.3 ± 4.8 mg/kg/min versus 7.4 ± 3.5 mg/kg/min; $P<0.05$), a 2-fold improvement in HGP suppression (77% versus 36%), and a 5-fold greater degree of FFA suppression (44% versus 8%) compared to their HFD-fed WT counterparts. The absolute rates of HGP and FFA levels in the basal state and at the end of the clamp studies are shown in Supplementary Fig. 4. We also measured fasted serum levels of insulin, and fed serum levels of adiponectin, FFA, glycerol, cholesterol, and triglycerides (Table 1). Fasting serum insulin levels were significantly lower in the HFD DT-treated CD11c-DTR BMT mice compared to their WT counterparts, consistent with the improvement in insulin sensitivity. It should be noted that metabolic improvement following DT treatment was seen as early as 24 hours. Although we did not measure CD11c+ cell content and inflammatory markers until 72 hours, previous studies have shown that DT treatment leads to near complete depletion of spleen and lymph node CD11c+ cells by 18 hours, accompanied by decreased infection-induced IL-12 levels (Liu et al., 2006;Probst et al., 2005).

Together, these data demonstrate that depletion of $CD11c^+$ cells leads to improved insulin sensitivity in both HFD-induced and a genetic model of obesity and insulin resistance, and that these insulin sensitizing effects occur in all major insulin-sensitive tissues (i.e. muscle, liver, and adipose tissue).

Ablation of CD11c-positive cells results in decreased expression of pro-inflammatory genes and increased expression of anti-inflammatory genes in AT from HFD-fed mice

Given that the $CD11c^+$ ATMs are important contributors to the increased expression of pro-inflammatory genes in obese AT (Lumeng et al., 2007; Nguyen et al., 2007), we quantified the expression of several of these genes in adipose tissue. As shown in Fig. 3a, HFD led to a 4-fold increase in the mRNA levels of the macrophage marker F4/80 in AT from DT-treated WT BMT mice, and this increase was markedly blunted in the HFD-fed, DT-treated CD11c-DTR BMT mice. These results are fully consistent with the decrease in ATMs that we observed upon $CD11c^+$ cell ablation as shown in Fig. 1b–d. Expression of the pro-inflammatory cytokine IL-6 and chemokine MCP-1 increased 4- and 10 fold, respectively, upon HFD feeding in WT BMT mice (Fig. 3b and c), whereas no increase was noted in AT from DT-treated CD11c-DTR BMT mice. Together, these results indicate that $CD11c^+$ cell depletion results in decreased pro-inflammatory responses in AT from HFD-fed mice. Interestingly, opposite directional changes were observed for the anti-inflammatory cytokine IL-10. In this case, HFD led to a small non-significant increase in AT from DT treated WT BMT mice, with a robust, highly significant increase in IL-10 mRNA expression in AT from the DT treated CD11c-DTR BMT group (Fig. 3d). These results suggest that the source of the IL-10 in the DT treated CD11c-DTR BMT mice are the remaining $CD11c^-$ ATMs (Cancello et al., 2005; Lumeng et al., 2007). The MCP-1 and IL-10 mRNA levels were confirmed at the protein level as shown in Fig. 3e, f.

Ablation of CD11c-positive cells results in decreased liver lipid levels

Since liver contains its own specialized resident macrophages (i.e. Kupffer cells) we analyzed whether DT treatment affected macrophage content in livers of CD11c-DTR BMT mice and their WT counterparts. $CD11c^+$ cell depletion did not affect hepatic macrophage content as measured by MAC2 IHC (Fig. 4a) and CD68 qPCR analysis (Fig. 4b).

Hepatic insulin resistance is usually accompanied by increased liver triglyceride (TG) content (Marchesini et al., 1999). We therefore measured liver TG levels and found a 45% reduction in HFD fed DT-treated CD11c-DTR BMT mice compared to their HFD WT counterparts (Fig. 4c). This is also illustrated by the decrease in lipid droplets in liver tissue sections (Fig. 4d). Since liver lipid content is regulated by both lipogenesis and lipid oxidation, we analyzed the expression of genes encoding liver X receptor α (LXRα), a key regulator of hepatic TG metabolism, its lipogenic target genes stearoyl CoA desaturase-1 (SCD1) and acetyl-CoA carboxylase 1 (ACC1), and peroxisome proliferator-activated receptor (PPAR) α, a key regulator of hepatic lipid oxidation (Lee et al., 2008; Sugden et al., 2002; Weickert and Pfeiffer, 2006). As shown in Fig. 4e, mRNA levels of the lipogenic genes LXRα, SCD1, and ACC1 were decreased in livers of HFD-fed DT-treated CD11c-DTR BMT mice while PPARα expression was unaffected. This was confirmed on the protein level for SCD1 and PPARα by Western blot (Fig. 4f). Furthermore, MCP-1 protein levels were decreased upon $CD11c^+$ cell ablation (Fig. 4f), suggesting that the inflammatory state of the liver is affected.

Together, these results show that, although $CD11c^+$ cell depletion does not affect liver Kupffer cell content, it does lead to a reduction in liver TG levels. This is most likely the result of decreased hepatic lipogenesis rather than increased lipid oxidation.

Ablation of CD11c-positive cells results in reduced muscle macrophage content, accompanied by decreased expression of inflammatory factors

We determined whether $CD11c^+$ cell depletion also affected skeletal muscle TG levels. As shown in Fig. 5a, HFD-feeding resulted in an increase in TG in quadriceps muscle, but no differences were observed between the two BM genotypes. We and others have previously shown that obesity is associated with increased macrophage content in skeletal muscle, including $CD11c^+$ cells, and this muscle macrophage accumulation is accompanied by

increased expression of inflammatory factors in muscle (Hevener et al., 2007;Nguyen et al., 2007;Weisberg et al., 2003). Therefore, we measured muscle mRNA levels of the macrophage marker CD68, and the inflammatory factors MCP-1 and TNF-α by qPCR. As shown in Fig. 5b–d, the expression of all three genes is increased by HFD-feeding in WT BMT mice but this increase is absent in DT treated CD11c-DTR BMT mice. Furthermore, protein levels of TNF-α, IL-6, and MCP-1 in muscle were decreased upon $CD11c^+$ cell ablation (Fig. 5e, f). These findings suggest that $CD11c^+$ cell depletion results in decreased skeletal muscle macrophage content with reduced expression of inflammatory factors. To verify the muscle macrophage content, we also performed MAC2 IHC. These results showed that muscle from obese animals was infiltrated and surrounded by adipose tissue that contained significant numbers of MAC2-positive macrophages (not shown), as was previously described (Weisberg et al., 2003). Furthermore, we observed MAC2-positive macrophages between muscle fibers at the outside borders of the quadriceps muscle tissue in HFD- but not in NC-fed mice (Fig. 5g, h). These MAC2-positive macrophages were absent in muscle from DT-treated HFD-fed CD11c-DTR BMT mice (Fig. 5i). Together, our results show that $CD11c^+$ cell depletion results in decreased skeletal muscle macrophage content and expression of inflammatory factors.

A clear relationship between increased intracellular muscle triglyceride (IMTG) accumulation and insulin resistance has been reported in obesity and type 2 diabetes (Moro et al., 2008). In the current study, $CD11c^+$ cell depletion reduced inflammatory markers in insulin target tissues, including muscle, suggesting that in this model increased IMTG content can be dissociated from insulin resistance in the absence of HFD-induced tissue inflammation.

Ablation of CD11c-positive cells results in reduced serum levels of inflammatory proteins

Next, we investigated whether our observations at the local tissue levels were also reflected in the serum levels of pro- and anti-inflammatory cytokines/chemokines. As shown in Fig. 6, serum levels of both pro- and anti-inflammatory cytokines were are all significantly reduced in the HFD-fed, DT-treated CD11c-DTR BMT mice compared to their WT counterparts. The lack of correlation between the IL-10 protein levels in serum and IL-10 mRNA and protein levels in AT agrees with previous findings showing that systemic IL-10 levels are not representative of the local inflammatory response (Hoedemaekers et al., 2005), and suggests that sources other than AT contribute to circulating IL-10.

In summary, we show that the conditional ablation of $CD11c^+$ cells leads to a marked reduction in adipose tissue and skeletal muscle macrophages in obese mice and that this $CD11c^+$ cell depletion results in both a local and systemic decrease in pro-inflammatory cytokine levels. This normalization of the inflammatory status is accompanied by a rapid and significant improvement of insulin sensitivity in AT, muscle, and liver.

Together, our results suggest that the $CD11c^+$ cells are an attractive target for development of new therapeutic approaches for treatment of obesity-related insulin resistance and type II diabetes.

EXPERIMENTAL PROCEDURES

Animals

Male C57BL/6J mice (3 months old) and male B6.V-Lep^{ob}/OlaHsd mice (6 weeks old) were acquired from Harlan and 8-week old male CD11c-DTR mice (B6.FVB-Tg(Itgax-DTR/EGFP) 57Lan/J) were purchased from Jackson Laboratories. To generate irradiated chimeras, mice received a lethal dose of 10 Gy radiation, followed by tail-vein injection of 3×10^6 bone marrow cells. Four to 6 weeks after the BMT, mice were bled to assess white blood cell number and differential by standard techniques (ACP Diagnostic Lab, University of California, San Diego).

Genomic DNA was extracted from the circulating blood leukocytes and genotyped by PCR to analyze reconstitution efficiency. After 6 weeks recovery on the NC diet, animals were either kept on NC (12% kcal from fat; Purina 5001, LabDiet) or fed a HFD (60% kcal from fat; D12492, Research Diets) for an additional 16 weeks. For systemic $CD11c^+$ cell depletion, CD11c-DTR BMT mice were injected i.p. with diphtheria toxin (in PBS; D0564; Sigma-Aldrich) at a dose of 10 ng/g body weight every other day for 3, 5, 9 or 17 days. As a negative control, WT BMT mice underwent the same treatment.

Mouse procedures conformed to the Guide for Care and Use of Laboratory Animals of the US National Institutes of Health, and were approved by the Animal Subjects Committee of the University of California, San Diego.

SVC isolation and FACS analysis

Epididymal fat pads were weighed, rinsed three times in PBS, and then minced in FACS buffer (PBS + 1 % low endotoxin BSA). Tissue suspensions were centrifuged at 500 *g* for 5 minutes and then collagenase-treated (1 mg/ml, Sigma-Aldrich) for 30 minutes at 37°C with shaking. Cell suspensions were filtered through a 100-μm filter and centrifuged at 500 *g* for 5 minutes. SVF pellets were then incubated with RBC Lysis Buffer (eBioscience) for 5 minutes prior to centrifugation (300 *g* for 5 minutes) and resuspension in FACS buffer.

Stromal vascular cells (SVCs) were incubated with Fc Block (BD Biosciences, San Jose, CA) for 20 minutes at 4°C prior to staining with fluorescently labeled primary antibodies or control IgGs, for 25 minutes at 4°C. F4/80-APC FACS antibody was purchased from AbD Serotec (Raleigh, NC); all other FITC- and PE-conjugated FACS antibodies were from BD Biosciences. Cells were gently washed twice and resuspended in FACS buffer with PI (Sigma-Aldrich). SVCs were analyzed using a FACSCalibur flow cytometer (BD Biosciences). Unstained, single stains and FMOs (fluorescence minus one) controls were used for setting compensation and gates.

IHC and quantification of CLS

Paraffin-imbedded adipose (epididymal), liver, and mucle (quadriceps) tissue sections from at least 5 mice per group were incubated with MAC-2 antibody (Cedarlane) at a 1:3800 dilution o/n at 4 degrees. Subsequently, a biotinylated anti-rat secondary antibody (Pharmingen) was used at 1:100 dilution, followed by 1:500 HRP-Streptavidin (Jackson) and development in substrate chromogen. Slides were counterstained with Mayer's and mounted with Vectashield mounting media with DAPI (Vector). Both brightfield (MAC-2) and fluorescent photographs (DAPI) were taken of 3 representative fields per slide in a blinded fashion using a fluorescent microscope (10x objective). The total number of nuclei per field were quantified by counting the DAPI-positive nuclei using ImageJ software (NIH freeware). MAC-2 positive CLS per field were counted manually and the number of CLS per 1000 nuclei per field was used as a measure of adipose tissue CLS content. For quantification of liver macrophage content we counted MAC-2 positive cells/field.

Metabolic studies

Glucose and insulin tolerance tests were performed on 6 hr fasted mice. For GTT, animals were injected ip with glucose (1 g/kg), whereas for ITT 0.75 (DIO model) or 1.5 (Ob/Ob) units/kg insulin (Novolin R, Novo-Nordisk) was injected ip. Blood samples were taken at 15, 30, 60, and 120 minutes after ip injection and glucose was measured using a One-Touch glucose-monitoring system (Lifescan).

Mouse euglycemic clamp studies were performed as previously described (Lesniewski et al., 2007). Briefly, dual jugular catheters were implanted and mice were allowed to recover 3 days

before clamp procedure. Following a 5 hr fast, an equilibrating solution was infused into one of the jugular catheters for 90 min to equilibrate the plasma with tracer (5 μCi/h of [3-^{3}H]D-glucose (NEN Life Science Products)). Following this equilibrating period, blood was sampled via a tail nick to obtain tracer counts for the calculation of basal glucose uptake, and to measure pre-clamp FFA levels. Following basal sampling, insulin (6.0 mU/kg/min, 0.12 ml/h) plus tracer (5 μCi/h) and glucose (50% dextrose, Abbot) infusions were started, with the glucose flow rate adjusted to reach a steady state blood glucose concentration (at ~120 min). Steady state was confirmed by stable tracer counts in plasma during final 30 min of clamp. An additional plasma sample was taken to measure post-clamp FFA levels. At steady state, the rate of glucose disappearance or the total GDR is equal to the sum of the rate of endogenous or HGP plus the exogenous (cold) glucose infusion rate. The IS-GDR is equal to the total GDR minus the basal glucose turnover rate.

Gene expression analyses

Total RNA was extracted from tissue with Trizol reagent following the supplier's protocol. Total RNA 2 μg was reverse-transcribed with using iScript cDNA Synthesis Kit (Bio- Rad Laboratories, Hercules, California, USA). Primer sequences used in the PCR reactions were chosen based on the sequences available in GenBank. Primers were designed to generate a PCR amplification product of 100–200 bp. Only primer pairs yielding unique amplification products without primer dimer formation were subsequently used for Q-PCR assays. Primer sequences are available upon request. PCR was carried out using iTaq SYBR Green supermix (Bio-Rad Laboratories, Hercules, California, USA) on an MJ Research Chromo4 Real Time PCR system (Bio-Rad Laboratories BV, Hercules, California, USA). The mRNA expression of all genes reported is normalized to the cyclophilin A gene expression.

Protein and lipid analyses

Plasma insulin levels were measured by ELISA (ALPCO). Plasma FFA levels were measured enzymatically using a commercially available kit (NEFA C; Wako Chemicals USA). Serum glycerol was measured using the Free Glycerol Reagent (Sigma). Triglycerides were measured using the Triglyceride-SL Assay (Diagnostic Chemicals Ltd.). Cholesterol was measured using the Chol kit and Roche/Hitachi analyzer (Roche). Cytokine/chemokine measurements in serum and tissue lysates were performed using two different 7-plex multiplex assays (Meso Scale Discovery, Millipore). Adiponectin serum levels were measured with a mouse adiponectin ELISA kit (BioSource). For Western blots we used an SCD1 antibody (Alexis), MCP-1 antibody (Abcam) and PPARα, TNFα, IL6 and β-tubulin antibodies (Santa Cruz).

Statistical analyses

All calculations were performed using PRISM 3.02 software (GraphPad, San Diego). Statistical significance between two groups was determined by the Student's *t* test. Comparisons among several groups were performed by ANOVA, and when the results passed the ANOVA test we performed Bonferroni's multiple comparison posttests to calculate the relevant *P*-values.

Supplementary Material

Refer to Web version on PubMed Central for supplementary material.

ACKNOWLEDGEMENTS

J.G.N. designed and initiated the study and completed the bone marrow transplantations, DT treatments, GTTs, ITTs, clamp studies, tissue harvests, immunohistological analyses, data analysis, and manuscript preparation as a member of J.M.O.'s laboratory. D.P. helped with bone marrow transplants, tissue harvests, immunohistological analyses, and

performed the qPCR gene expression analysis, muscle triglyceride measurements, skeletal muscle Western blots, and prepared tissue lysates. P.P.L. helped with bone marrow transplants and clamps and prepared SVFs for FACS analyses and performed serum glycerol measurements and liver Western blots. D.T and J.C. performed the serum cytokine measurements. J.M.O. provided scientific advice and guidance.

We thank J. Juliano for the serum and liver cholesterol and triglyceride measurements, J. M. Ofrecio for serum insulin and FFA measurements, D. D. Sears for help in facilitating the cytokine measurements, C. Castorena for technical assistance, and S. Schenk and M. Saberi for help with mouse tail vein injections. At the Rebecca & John Moores UCSD Cancer Center, we thank the Flow Cytometry Resource and D.J. Young for his assistance with FACS analysis, and the Histology and Immunohistochemistry Resource (L. Gapuz and N. Varki). Support for this research was provided by NIH DK033651, DK 074868 and HD 012303, as well as a UC Discovery BioStar grant to J.M.O, and a Scientist Development Grant from the American Heart Association (0635408N) and an Inserm Junior Researchers Temporary contract to J.G.N.

REFERENCES

Arkan MC, Hevener AL, Greten FR, Maeda S, Li ZW, Long JM, Wynshaw-Boris A, Poli G, Olefsky J, Karin M. IKK-beta links inflammation to obesity-induced insulin resistance. Nat Med 2005;11:191–198. [PubMed: 15685170]

Brake DK, Smith EO, Mersmann H, Smith CW, Robker RL. ICAM-1 expression in adipose tissue: effects of diet-induced obesity in mice. Am J Physiol Cell Physiol 2006;291:C1232–C1239. [PubMed: 16807303]

Cancello R, Henegar C, Viguerie N, Taleb S, Poitou C, Rouault C, Coupaye M, Pelloux V, Hugol D, Bouillot JL, et al. Reduction of macrophage infiltration and chemoattractant gene expression changes in white adipose tissue of morbidly obese subjects after surgery-induced weight loss. Diabetes 2005;54:2277–2286. [PubMed: 16046292]

Cinti S, Mitchell G, Barbatelli G, Murano I, Ceresi E, Faloia E, Wang S, Fortier M, Greenberg AS, Obin MS. Adipocyte death defines macrophage localization and function in adipose tissue of obese mice and humans. J Lipid Res 2005;46:2347–2355. [PubMed: 16150820]

Ellacott KL, Murphy JG, Marks DL, Cone RD. Obesity-induced inflammation in white adipose tissue is attenuated by loss of melanocortin-3 receptor signaling. Endocrinology 2007;148:6186–6194. [PubMed: 17901224]

Gordon S, Taylor PR. Monocyte and macrophage heterogeneity. Nat Rev Immunol 2005;5:953–964. [PubMed: 16322748]

Hevener AL, Olefsky JM, Reichart D, Nguyen MT, Bandyopadyhay G, Leung HY, Watt MJ, Benner C, Febbraio MA, Nguyen AK, et al. Macrophage PPAR gamma is required for normal skeletal muscle and hepatic insulin sensitivity and full antidiabetic effects of thiazolidinediones. J Clin Invest 2007;117:1658–1669. [PubMed: 17525798]

Hirasaka K, Kohno S, Goto J, Furochi H, Mawatari K, Harada N, Hosaka T, Nakaya Y, Ishidoh K, Obata T, et al. Deficiency of Cbl-b gene enhances infiltration and activation of macrophages in adipose tissue and causes peripheral insulin resistance in mice. Diabetes 2007;56:2511–2522. [PubMed: 17601987]

Hoedemaekers CW, Pickkers P, Netea MG, van Deuren M, Van der Hoeven JG. Intensive insulin therapy does not alter the inflammatory response in patients undergoing coronary artery bypass grafting: a randomized controlled trial [ISRCTN95608630]. Crit Care 2005;9:R790–R797. [PubMed: 16356228]

Jung S, Unutmaz D, Wong P, Sano G, De los Santos K, Sparwasser T, Wu S, Vuthoori S, Ko K, Zavala F, et al. In vivo depletion of CD11c(+) dendritic cells abrogates priming of CD8(+) T cells by exogenous cell-associated antigens. Immunity 2002;17:211–220. [PubMed: 12196292]

Kamei N, Tobe K, Suzuki R, Ohsugi M, Watanabe T, Kubota N, Ohtsuka-Kowatari N, Kumagai K, Sakamoto K, Kobayashi M, et al. Overexpression of monocyte chemoattractant protein-1 in adipose tissues causes macrophage recruitment and insulin resistance. J Biol Chem 2006;281:26602–26614. [PubMed: 16809344]

Kanda H, Tateya S, Tamori Y, Kotani K, Hiasa K, Kitazawa R, Kitazawa S, Miyachi H, Maeda S, Egashira K, Kasuga M. MCP-1 contributes to macrophage infiltration into adipose tissue, insulin resistance, and hepatic steatosis in obesity. J Clin Invest 2006;116:1494–1505. [PubMed: 16691291]

Lee JH, Zhou J, Xie W. PXR and LXR in hepatic steatosis: a new dog and an old dog with new tricks. Mol Pharm 2008;5:60–66. [PubMed: 18072748]

Lesniewski LA, Hosch SE, Neels JG, de Luca C, Pashmforoush M, Lumeng CN, Chiang SH, Scadeng M, Saltiel AR, Olefsky JM. Bone marrow-specific Cap gene deletion protects against high-fat diet-induced insulin resistance. Nat Med 2007;13:455–462. [PubMed: 17351624]

Liu CH, Fan YT, Dias A, Esper L, Corn RA, Bafica A, Machado FS, Aliberti J. Cutting edge: dendritic cells are essential for in vivo IL-12 production and development of resistance against Toxoplasma gondii infection in mice. J Immunol 2006;177:31–35. [PubMed: 16785494]

Lumeng CN, Bodzin JL, Saltiel AR. Obesity induces a phenotypic switch in adipose tissue macrophage polarization. J Clin Invest 2007;117:175–184. [PubMed: 17200717]

Mantovani A, Sica A, Sozzani S, Allavena P, Vecchi A, Locati M. The chemokine system in diverse forms of macrophage activation and polarization. Trends Immunol 2004;25:677–686. [PubMed: 15530839]

Marchesini G, Brizi M, Morselli-Labate AM, Bianchi G, Bugianesi E, McCullough AJ, Forlani G, Melchionda N. Association of nonalcoholic fatty liver disease with insulin resistance. Am J Med 1999;107:450–455. [PubMed: 10569299]

Moro C, Bajpeyi S, Smith SR. Determinants of intramyocellular triglyceride turnover: implications for insulin sensitivity. Am J Physiol Endocrinol Metab 2008;294:E203–E213. [PubMed: 18003718]

Nara N, Nakayama Y, Okamoto S, Tamura H, Kiyono M, Muraoka M, Tanaka K, Taya C, Shitara H, Ishii R, et al. Disruption of CXC motif chemokine ligand-14 in mice ameliorates obesity-induced insulin resistance. J Biol Chem 2007;282:30794–30803. [PubMed: 17724031]

Neels JG, Olefsky JM. Inflamed fat: what starts the fire? J Clin Invest 2006;116:33–35. [PubMed: 16395402]

Nguyen MT, Favelyukis S, Nguyen AK, Reichart D, Scott PA, Jenn A, Liu-Bryan R, Glass CK, Neels JG, Olefsky JM. A subpopulation of macrophages infiltrates hypertrophic adipose tissue and is activated by free fatty acids via Toll-like receptors 2 and 4 and JNK-dependent pathways. J Biol Chem 2007;282:35279–35292. [PubMed: 17916553]

Nomiyama T, Perez-Tilve D, Ogawa D, Gizard F, Zhao Y, Heywood EB, Jones KL, Kawamori R, Cassis LA, Tschop MH, Bruemmer D. Osteopontin mediates obesity-induced adipose tissue macrophage infiltration and insulin resistance in mice. J Clin Invest 2007;117:2877–2888. [PubMed: 17823662]

Probst HC, Tschannen K, Odermatt B, Schwendener R, Zinkernagel RM, Van Den Broek M. Histological analysis of CD11c-DTR/GFP mice after in vivo depletion of dendritic cells. Clin Exp Immunol 2005;141:398–404. [PubMed: 16045728]

Shoelson SE, Herrero L, Naaz A. Obesity, inflammation, and insulin resistance. Gastroenterology 2007;132:2169–2180. [PubMed: 17498510]

Solinas G, Vilcu C, Neels JG, Bandyopadhyay GK, Luo JL, Naugler W, Grivennikov S, Wynshaw-Boris A, Scadeng M, Olefsky JM, Karin M. JNK1 in hematopoietically derived cells contributes to diet-induced inflammation and insulin resistance without affecting obesity. Cell Metab 2007;6:386–397. [PubMed: 17983584]

Strissel KJ, Stancheva Z, Miyoshi H, Perfield JW 2nd, Defuria J, Jick Z, Greenberg AS, Obin MS. Adipocyte Death, Adipose Tissue Remodeling and Obesity Complications. Diabetes. 2007

Sugden MC, Bulmer K, Gibbons GF, Knight BL, Holness MJ. Peroxisome-proliferator-activated receptor-alpha (PPARalpha) deficiency leads to dysregulation of hepatic lipid and carbohydrate metabolism by fatty acids and insulin. Biochem J 2002;364:361–368. [PubMed: 12023878]

Weickert MO, Pfeiffer AF. Signalling mechanisms linking hepatic glucose and lipid metabolism. Diabetologia 2006;49:1732–1741. [PubMed: 16718463]

Weisberg SP, Hunter D, Huber R, Lemieux J, Slaymaker S, Vaddi K, Charo I, Leibel RL, Ferrante AW Jr. CCR2 modulates inflammatory and metabolic effects of high-fat feeding. J Clin Invest 2006;116:115–124. [PubMed: 16341265]

Weisberg SP, McCann D, Desai M, Rosenbaum M, Leibel RL, Ferrante AW Jr. Obesity is associated with macrophage accumulation in adipose tissue. J Clin Invest 2003;112:1796–1808. [PubMed: 14679176]

Zammit DJ, Cauley LS, Pham QM, Lefrancois L. Dendritic cells maximize the memory CD8 T cell response to infection. Immunity 2005;22:561–570. [PubMed: 15894274]

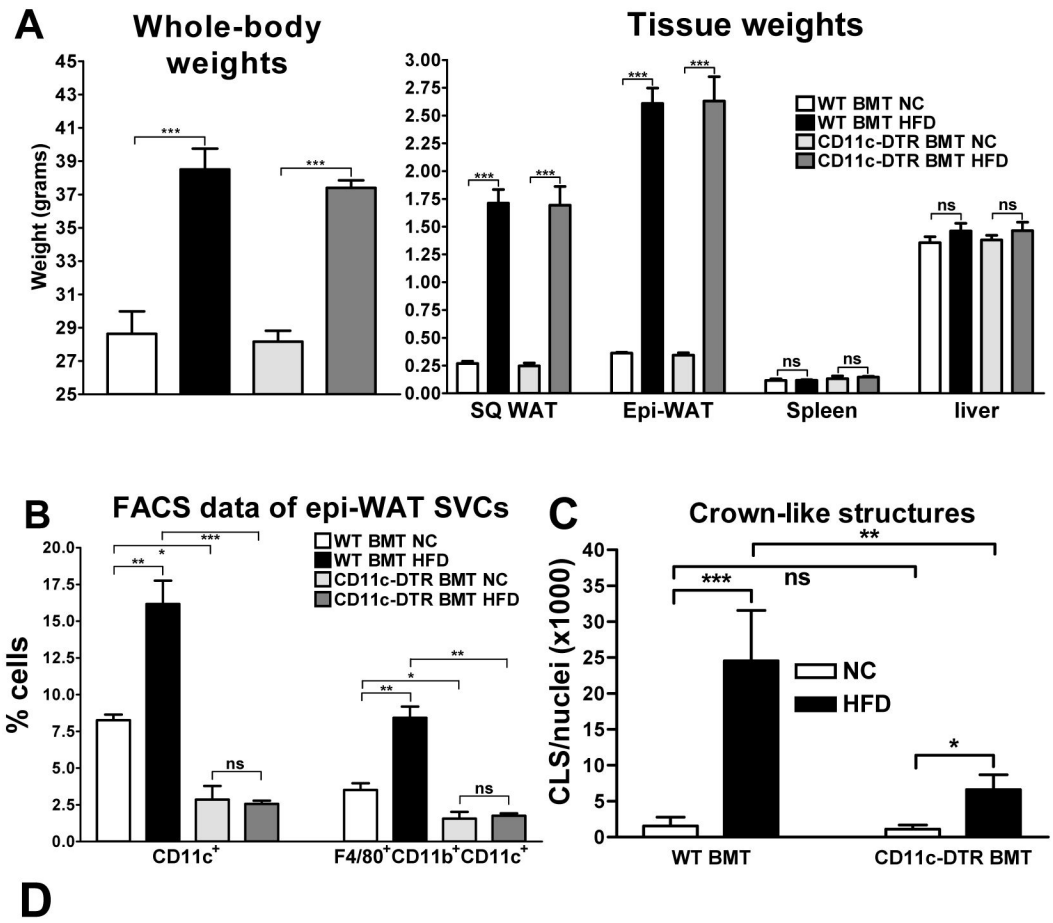

Figure 1. Ablation of CD11c$^+$ cells leads to a reduction of crown-like structures in epi-WAT

a) Whole-body (left) and tissue weights (right) in grams of both WT BMT and CD11c-DTR BMT mice fed NC or HFD. Whole-body weights were measured before DT treatment and tissue weights were measured after DT treatment at time of sacrifice. **b**) SVFs were extracted from the epi-WAT samples. The SVCs were subsequently stained for F4/80, CD11b, and CD11c cell surface proteins and analyzed by FACS. The number of CD11c$^+$ and F4/80$^+$CD11b$^+$CD11c$^+$ cells is indicated as percentage of total SVCs. **c**) Paraffin-imbedded epi-WAT sections were stained for MAC-2. Stained slides were subsequently coverslipped with DAPI-containing mounting media and brightfield (MAC-2) and fluorescent (DAPI) images were taken of 3 representative fields per slide in a blinded fashion using a fluorescent

microscope (10 × objective). Nuclei per field were quantified by counting DAPI-positive nuclei using ImageJ software. MAC-2 positive crown-like structures (CLS) per field were counted manually and the number of CLS per 1000 nuclei was used as another measure of adipose tissue macrophage content. **d**) Examples of MAC2 immunohistochemistry as quantified in **panel c**. MAC2-stained cells (brown) surrounding adipocytes form the CLS. Scale bar represents 250 μm. All data shown in this figure were combined from 4 groups of mice that were treated with DT for a period of 3, 5, 9, or 17 days. Data are expressed as mean ± SEM. **P*<0.05; ***P*<0.01; *** *P*<0.001; ns means not significant; $n \geq 15$ per group.

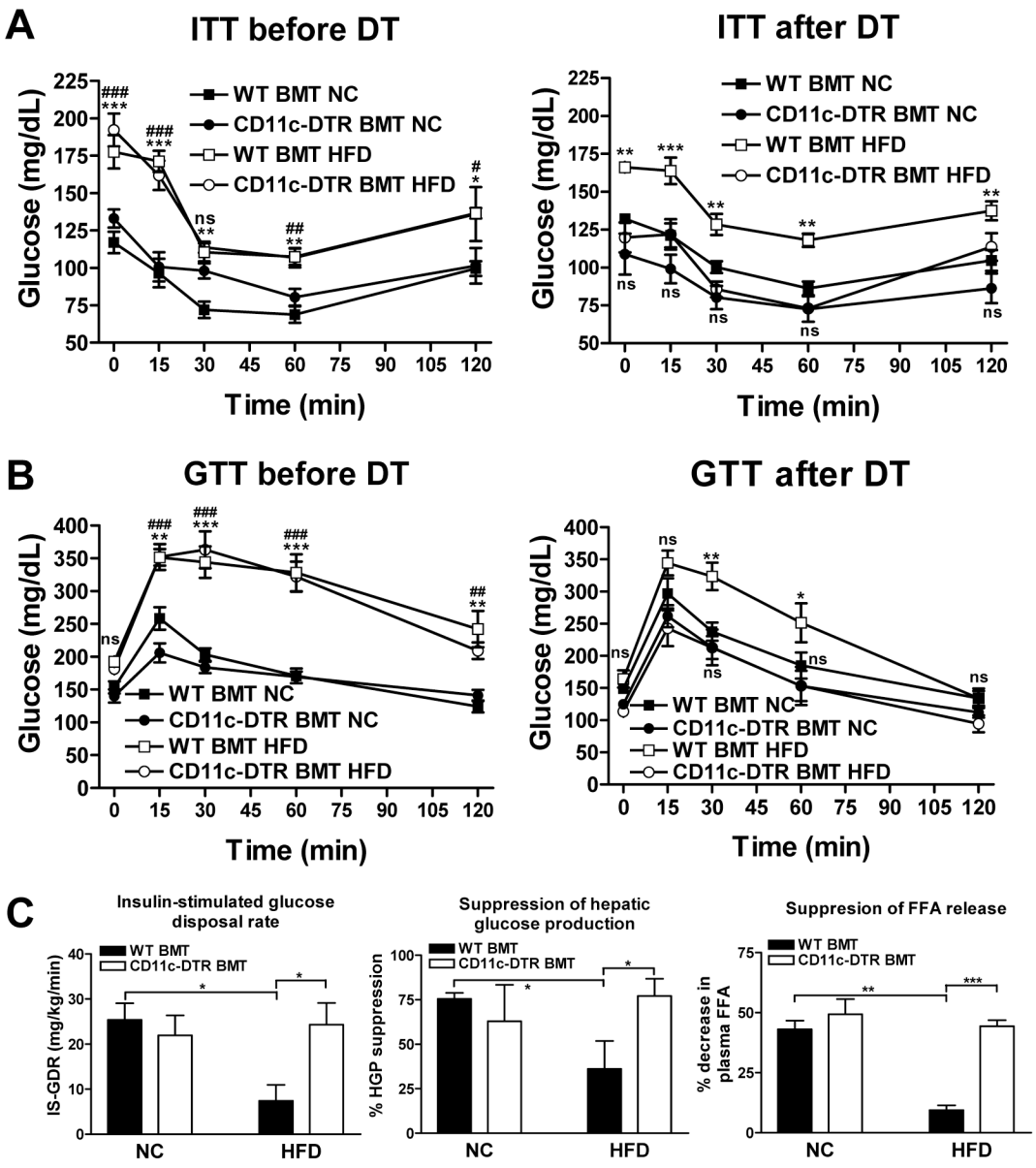

Figure 2. Metabolic studies

In vivo glucose homeostasis as determined by ITTs (**a**) or GTTs (**b**) before (left) and 24-hrs after (right) a single dose of DT treatment. Data are expressed as mean ± SEM, $n = 5$ per group. *$P<0.05$. **$P<0.01$, *** $P<0.001$, and ns means not significant when comparing WT BMT HFD versus WT BMT NC. $^{\#}P<0.05$. $^{\#\#}P<0.01$, $^{\#\#\#}P<0.001$, and ns means not significant when comparing CD11c-DTR BMT HFD versus CD11c-DTR BMT NC. **c**) *In vivo* insulin sensitivity as determined by euglycemic clamp studies in NC- and HFD-fed WT and CD11c-DTR BMT mice treated with DT. IS-GDR (left) is indicative of insulin sensitivity in skeletal muscle, liver insulin sensitivity is reflected by suppression of hepatic glucose production (middle), and suppression of plasma free fatty acids is a measure for adipose insulin sensitivity (right). NC data was from mice treated with DT for 14 days. HFD data was combined from 3 sets of mice that received DT for 1, 3, or 7 days. Data are expressed as mean ± SEM. *$P<0.05$, **$P<0.01$ and *** $P<0.001$. n=5 per group for NC data and $n \geq 15$ per group for HFD data.

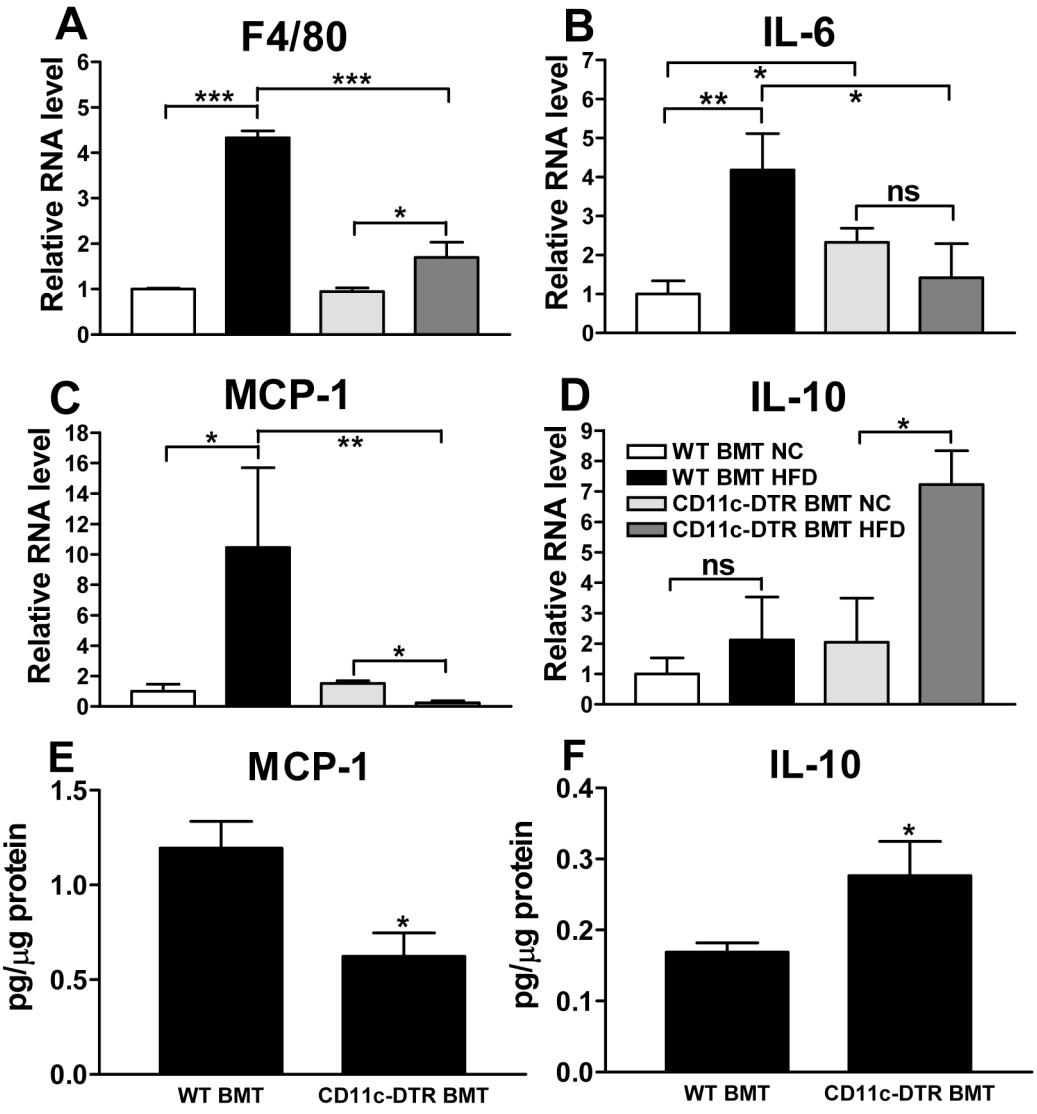

Figure 3. WAT mRNA and protein levels

Gene expression in adipose tissue from mice treated with DT for 9 days was analyzed by measuring relative mRNA levels using qPCR for **a**) the macrophage marker F4/80, **b**) the pro-inflammatory cytokine IL-6, **c**) the pro-inflammatory chemokine and macrophage chemoattractant MCP-1, and **d**) the anti-inflammatory cytokine IL-10. The protein levels of **e**) MCP-1 and **f**) IL-10 were measured in adipose tissues lysates of HFD-fed WT and CD11c-DTR BMT mice. Data are expressed as mean ± SEM. **P*<0.05; ***P*<0.01; ****P*<0.001; ns means not significant. $n \geq 4$ per group.

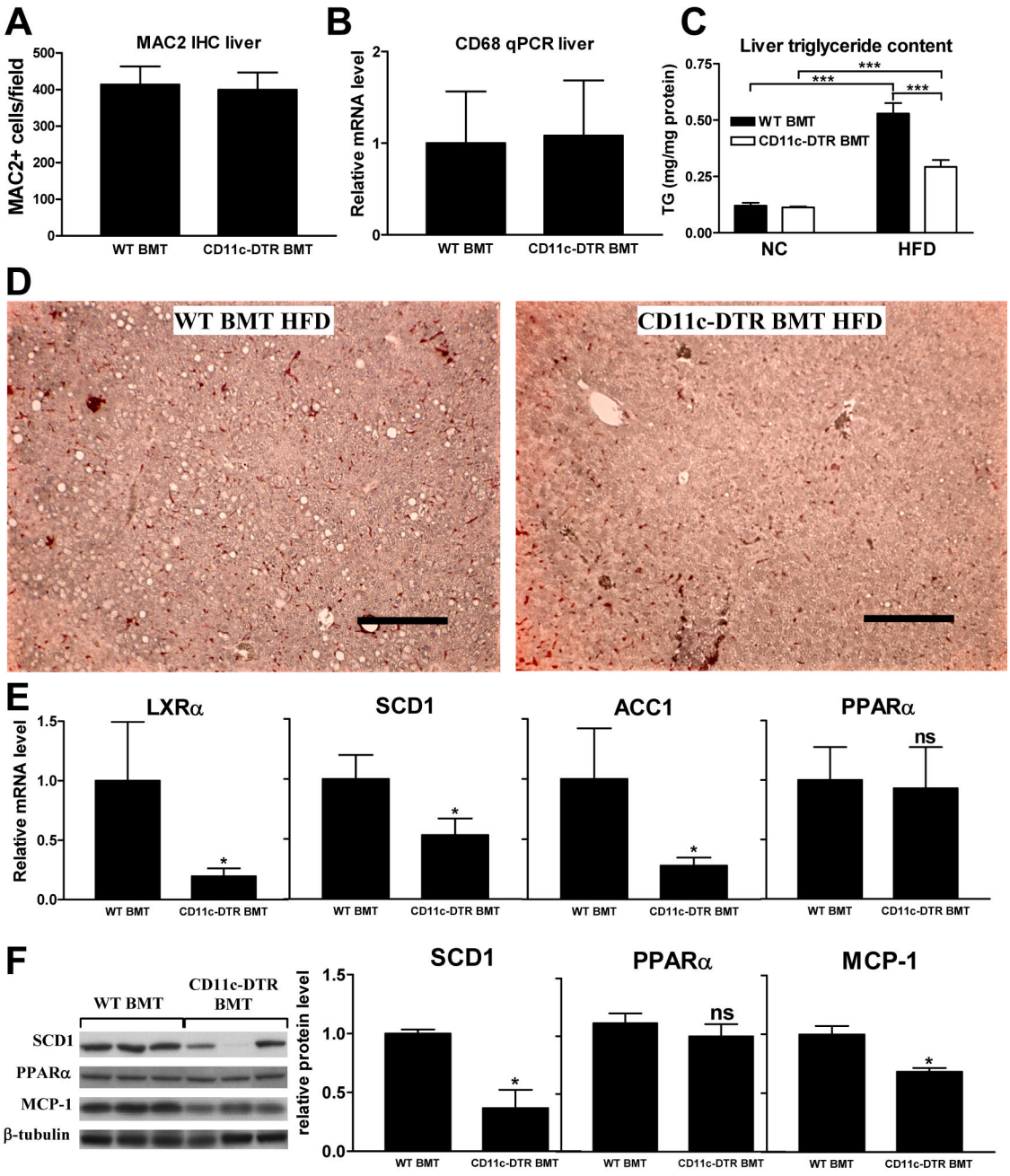

Figure 4. Liver data

Liver macrophage content as measured by quantification of **a)** MAC2 immunohistochemistry and **b**) relative mRNA levels of the macrophage marker CD68. **c**) Liver triglyceride content as measured in liver lysates and **d**) as illustrated by presence of clear lipid droplets in MAC2-stained liver tissue sections. Scale bar represents 250 μm. **e**) Relative liver mRNA levels of liver X receptor alpha (LXRα), stearoyl CoA desaturase-1 (SCD1), acetyl-CoA carboxylase 1 (ACC1), and peroxisome proliferator-activated receptor (PPAR) α. **f**) Western blots for SCD1, PPARα, MCP-1 and β-tubulin showing relative protein levels normalized to β-tubulin. All data shown in this figure were combined from 4 groups of mice that were treated with DT for a period of 3, 5, 9, or 17 days. Data are expressed as mean ± SEM. **P*<0.05 compared to WT BMT. ****P*<0.001. $n \geq 15$ per group. ns means not significant.

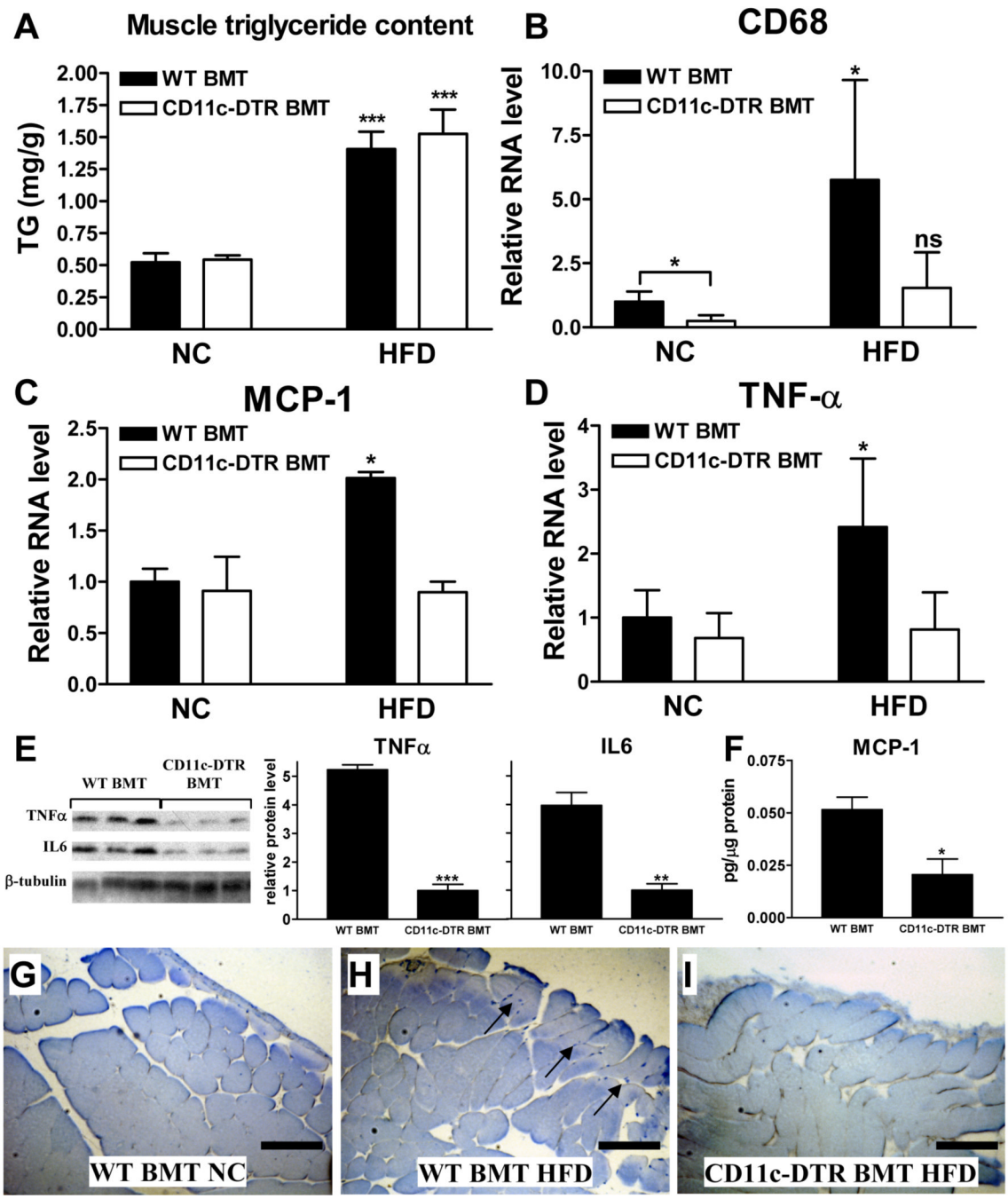

Figure 5. Muscle data

a) Triglyceride levels in quadriceps muscles. **b**) Muscle macrophage content as quantified by determining the relative mRNA level of the macrophage marker CD68 by qPCR. Relative mRNA levels of the inflammatory factors **c**) MCP-1 and **d**) TNF-α in quadriceps muscles as determined by qPCR. Protein levels of **e**) TNFα and IL6 measured by Western blot and **f**) MCP-1 measured by multiplex ELISA in skeletal muscle tissue lysates of HFD-fed WT and CD11c-DTR BMT mice. Western blot data were expressed as relative protein level normalized to β-tubulin. MAC2-stained muscle section of a **g**) NC-fed WT BMT mouse, **h**) a HFD-fed WT BMT mouse, and **i**) a HFD-fed CD11c-DTR mouse. The arrows in **panel h** point towards tissue areas where MAC2-positive macrophages are visible (blue staining). Scale bar represents

250 μm. The quadriceps muscles were obtained from a group of mice that was treated with DT for a period of 9 days and the data are expressed as mean ± SEM. *P<0.05, ** P<0.01, ***P<0.001, and ns means not significant when compared to NC-fed or WT counterpart. n=5 per group.

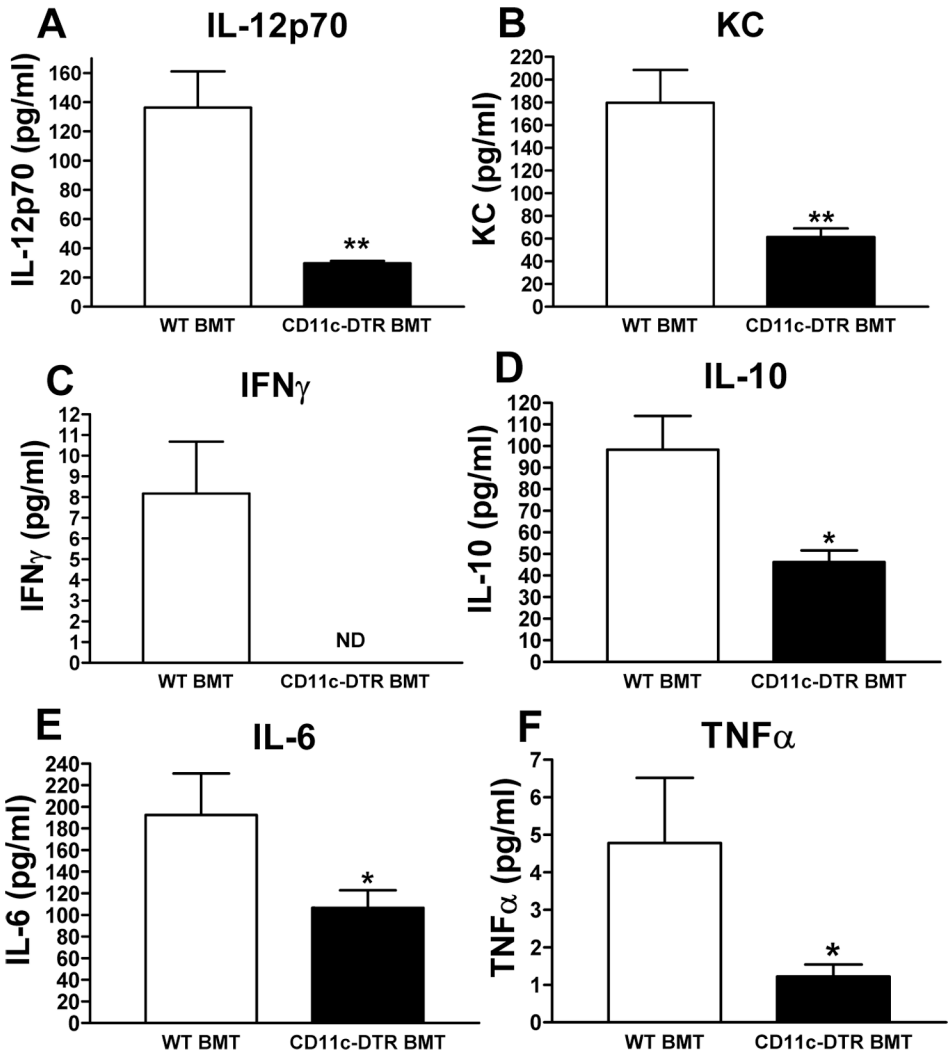

Figure 6. Serum cytokine/chemokine measurements

Multiplex ELISA was used to measure the concentration of **a**) IL-12p70, **b**) keratinocyte-derived chemokine (KC), **c**) interferon γ (IFNγ), **d**) IL-10, **e**) IL-6, and **f**) TNF-α in serum of HFD-fed, DT treated CD11c-DTR BMT mice and their WT counterparts. Data are expressed as mean ± SEM and was combined from 4 groups of mice that were treated with DT for a period of 3, 5, 9, or 17 days. **P*<0.05; ***P*<0.01; ND means not detectable. *n* = 12 per group.

Table 1

Metabolic parameters

Diet	Normal chow		High fat diet	
BM genotype	**WT**	**CD11c-DTR**	**WT**	**CD11c-DTR**
Serum insulin (ng/ml)	1.12 ± 0.14	1.14 ± 0.20	6.32 ± 1.26$^{\#\#\#}$	2.79 ± 0.37**
Serum FFA levels (mmol/L)	0.70 ± 0.12	0.61 ± 0.12	1.12 ± 0.20	0.98 ± 0.15
Serum glycerol levels (μg/ml)	28.13 ± 5.24	23.5 ± 3.18	69.67 ± 15.37$^{\#}$	62.83 ± 11.71$^{\#}$
Serum adiponectin levels (μg/ml)	30.84 ± 1.92	30.61 ± 1.60	34.86 ± 2.69	34.06 ± 2.89
Serum cholesterol levels (mg/dL)	77.4 ± 3.8	71.7 ± 1.2	173.5 ± 13.8$^{\#\#\#}$	145.9 ± 8.3$^{\#\#\#}$
Liver cholesterol levels (mg/mg protein)	0.18 ± 0.004	0.18 ± 0.013	0.18 ± 0.010	0.17 ± 0.007
Serum triglyceride levels (mg/dL)	113.2 ± 12.2	105.7 ± 19.4	154.3 ± 16.1	138.7 ± 36.6

Data are expressed as mean ± SEM.

*Significant difference between BM genotype within diet.

$^{\#}$Significant difference between diet within genotype.

*$P<0.05$;

**$P<0.01$;

***$P<0.001$.

$^{\#}$$P<0.05$.

$^{\#\#}$$P<0.01$

$^{\#\#\#}$$P<0.001$.

$n \geq 12$ per group.